nature medicine

Article

https://doi.org/10.1038/s41591-025-03919-w

Oligodendrocyte-targeted adeno-associated virus gene therapy for Canavan disease in children: a phase 1/2 trial

Received: 31 December 2024

Accepted: 25 July 2025

Published online: 16 September 2025

Check for updates

Paola Leone[1,6], Robert M. Lober[2,3,6], Jeremy Francis[1], Olga Flamini[4] ✉, Kim M. Cecil[5], David Shera[4] & Christopher G. Janson[1,2,3] ✉

This open-label phase 1/2 clinical study uses a novel recombinant vector, rAAV-Olig001, with selective tropism for oligodendrocytes, to deliver gene therapy for Canavan disease (CD), a rare leukodystrophy characterized by defective aspartoacylase and elevated *N*-acetyl-aspartic acid (NAA) concentrations. A total of 8 participants received intracranial doses of 3.7×10^{13} vector genomes (vg) of rAAV-Olig001-ASPA (MYR-101), with an interim analysis at 12 months. The primary objective was to assess the safety of intracranial dosing of MYR-101 in children with typical CD. Efficacy measures included Mullen Scales of Early Learning (MSEL), Gross Motor Function Measure (GMFM) and analysis of NAA, myelination, white matter and extracellular water content in the brain. The participants were White; 5 (62.5%) were male. Of the participants, 7 (87.5%) experienced ≥1 serious adverse event, none of which were considered MYR-101 related. All participants experienced ≥1 adverse event. All adverse events and serious adverse events resolved fully. Treatment reduced NAA concentrations in cerebrospinal fluid ($P = 0.0008$), increased myelination ($P = 0.0137$) and improved MSEL developmental outcomes ($P = 0.0171$). Thus, interim results suggest that gene therapy with MYR-101 is well tolerated and shows early effects in CD. While these findings are preliminary, reductions in NAA concentrations indicate *ASPA* expression and increases in myelination and imply successful targeting of oligodendrocytes. These results may support the development of similar gene therapy strategies for other demyelinating and metabolic brain disorders. ClinicalTrials.gov registration: NCT04833907.

Canavan disease (CD) is a rare autosomal recessive leukodystrophy characterized by spongiform degeneration of white matter in the brain. The eponym refers to neuropathologist Myrtelle Canavan, who described the affected brain pathology as 'subcortical loss of myelin with a diffuse and marked edema of the white matter'[1]. CD is caused by mutations in the *ASPA* gene, which encodes the aspartoacylase (ASPA) enzyme responsible for metabolizing the substrate molecule, *N*-acetyl-aspartic acid (NAA). Lack of functional ASPA and the resulting increase in the concentration of NAA in the central nervous system impair normal myelination and result in dysmyelination and progressive degradation of the brain's white matter and myelin, with relative sparing of neurons[2,3]. The harmful effect of high interstitial concentrations of NAA is thought to be multifactorial, encompassing metabolic, osmotic and possibly cytotoxic effects[3–7]. Two forms of CD have been observed. In the neonatal/infantile-onset form (also called typical CD), which is the most common form, the signs manifest by 3 months to

A full list of affiliations appears at the end of the paper. ✉e-mail: OFlamini@MyrtelleGTX.com; janson@memorymatters.org

6 months of age. In the less common juvenile-onset form (also called atypical), the disease is apparent in the first years of life[8,9].

The neonatal/infantile-onset form results in severe disease[10–12] but shows no obvious phenotypical abnormalities at birth[6,7,13]. Signs develop within the first 6 months of life and invariably worsen over time. The disease manifests initially with hypotonia, poor head control, delayed cognitive responses and macrocephaly. With increasing age, patients may become irritable, lethargic and listless, and experience sleep disturbance. They also commonly have poor visual tracking or blindness, seizures and feeding difficulties. Seizures are a frequent early manifestation, which may be absence, myoclonic or generalized tonic–clonic. Eventually, patients experience life-threatening complications such as psychomotor arrest and hydrocephalus[3,6,7].

The milder atypical variant of CD presents later and with milder symptoms such as speech and minor motor delays, often not affecting lifespan[8,9]. These atypical cases, which show divergent scores on the Gross Motor Function Measure-88 (GMFM-88), are excluded from our study to ensure a homogenous study population that is more representative of the disease's severe impact. Previous studies showed low ASPA enzyme activity in atypical mild-onset cases of CD, with recent data indicating activity between 10% and 35% of normal. By contrast, typical CD shows <5% of normal ASPA enzyme activity[8,14,15]. This suggests that even a modest increase in ASPA enzyme could potentially alter the clinical phenotype in typical CD.

Given its well-defined genetic defect, devastating clinical course and lack of any proven disease-modifying therapy, CD has been a compelling candidate for neurological gene therapy. Our team developed CD gene therapy over 25 years ago, using nonviral and early recombinant adeno-associated virus (rAAV) vectors[2,16]. While neuron-targeted rAAV reduced NAA concentrations in the brain, it failed to improve long-term myelination or psychomotor function[17]. To address this, a novel rAAV vector was developed with specific tropism for oligodendrocytes, the primary cells affected in CD, based on the hypothesis that targeting oligodendrocytes would result in greater myelination than standard targeting of neurotropic or astroglial cells and would improve clinical outcomes[5].

Preclinical data for this first-in-human (FIH) study were obtained using Nur7 mice, a well-characterized and publicly available null *ASPA* mouse model of CD with an inactive ASPA enzyme caused by a Q193X nonsense mutation in the *ASPA* gene. Unlike other animal models of the disease, the Nur7 mouse[5,18–22] effectively replicates human pathology primarily restricted to the brain, characterized by inactive ASPA enzyme, elevated NAA concentrations, dysmyelination, spongy degeneration, vacuolation and motor deficits. Efficacy and safety studies of rAAV-Olig001-ASPA (MYR-101), a vector designed to restore *ASPA* expression in oligodendrocytes, showed that intracranial doses reversed behavioral and pathological features of CD in symptomatic 12-week-old Nur7 mice[5,18]. MYR-101 showed no toxicity or microscopic pathology in major organs. MYR-101-treated Nur7 mice had significantly improved motor function and significantly lower NAA concentrations in the brain compared with controls[18], outperforming an AAV9-ASPA comparator, in a dose-dependent manner due to oligodendrocyte-specific tropism[18].

Here we present preliminary safety and efficacy data for the first 8 participants at the 12-month data interim analysis. Two different production runs of vector were used for the first 8 participants. The first production run of vector was used for the first three participants (001, 002, 003), and the second production run of vector was used for the next five participants (004, 009, 028, 031, 032). Due to a delay in clinical vector batch release, the first 3 participants have 24-month data and 4 participants have 12-month data. One foreign participant was unable to return for scheduled in-person assessments owing to visa restrictions but remains under follow-up for safety monitoring remotely.

Our clinical protocol compared neurological development in participants treated with MYR-101 to that of age-matched patients for whom natural history (NH) data are available. We also assessed longitudinal changes from baseline in key biomarkers for CD, including cerebrospinal fluid (CSF) NAA, brain myelin and water content.

Table 1 | Participant demographics

Participant identifier	Age (months) at treatment	Sex	Country of origin	*ASPA* mutation
001	57	M	United States	854A>C 854A>C
002	47	M	United States	854A>C 854A>C
003	48	F	Italy	503G>A 542C>G
004	59	M	Russia	634+1G>T 914C>A
009	18	F	United States	503G>A 914C>A
028	39	F	Slovakia	693C>T 854A>C
031	12	M	Chile	426C>A 59C>T
032	19	M	Argentina	557T>A 838C>T

Results

All eight participants had confirmed pathological gene mutations consistent with severe typical CD (Table 1), and have low functional scores at baseline characteristic of typical CD. The male to female ratio was 5:3. All participants were White and two were of Jewish descent. The majority of participants presented with mutations typical of Jewish founders. None of the participants had other genetic diseases or concurrent conditions that would disqualify them from the study.

Safety

All 8 of the initial MYR-101-treated participants in this interim report experienced an adverse event (AE); a total of 73 AEs were reported (Table 2). Of the 8 participants, 7 (87.5%) experienced at least one serious AE (SAE), but none of these SAEs were related to the MYR-101 drug product. Procedure-related SAEs included seizures and CSF leakage. No fatalities occurred over the course of the study. Two non-SAEs in one participant (moderate fever and mild rash that subsequently resolved) were considered possibly related to MYR-101 treatment. One participant experienced transient pancytopenia 2 months after the treatment, which was related to an intercurrent viral illness. Several participants experienced common pediatric viral pulmonary infections, including COVID-19 during the pandemic, but none of the infections were treatment related. Participants with CD frequently experience aspiration events and are ordinarily at high risk for infections[13]. In terms of other neurological complications, a single case of seizure cluster was observed. The participant (002) experienced a total of 6 episodes of seizure between days 206 and 466.

Clinical assessments

NAA in CSF assessed by mass spectrometry. To assess how treatment with MYR-101 affects NAA concentration in the CSF, we directly sampled CSF before and after treatment and measured NAA using mass spectrometry. One participant's family refused CSF collection after treatment; hence, CSF data for seven of the eight participants were available for analysis. We observed a greater than 80% reduction in NAA concentration across all participants (Fig. 1a). We used a two-sided *t*-test to compare baseline and posttreatment NAA values, which revealed a substantial drop in NAA concentrations across all participants ($P = 0.0008$) (Fig. 1b). NAA levels in the CSF are proportional to levels in the interstitial space, although there is an approximately

https://doi.org/10.1038/s41591-025-03919-w

Table 2 | Adverse events for MYR-101-treated participants

	Participants, *n* (%)
Participants with any adverse events	8/8 (100)
Participants with any SAE	7/8 (87.5)
Total number of adverse events	73
Infections and infestations	
COVID-19	4/8 (50.0)
Pneumonia	3/8 (37.5)
Respiratory syncytial virus infection	2/8 (25.0)
Asymptomatic COVID-19	1/8 (12.5)
Bronchiolitis	1/8 (12.5)
Strep pharyngitis	1/8 (12.5)
Pneumonia aspiration	1/8 (12.5)
Rhinovirus or enterovirus infection	1/8 (12.5)
Gastrointestinal disorders	
Dental caries	2/8 (25.0)
Dysphagia	3/8 (37.5)
Abdominal pain	1/8 (12.5)
Constipation	1/8 (12.5)
Umbilical hernia	1/8 (12.5)
Vomiting	1/8 (12.5)
Nervous system disorders	
Seizure	5/8 (62.5)
Autonomic nervous system imbalance	1/8 (12.5)
CSF leakage	1/8 (12.5)
Seizure cluster	1/8 (12.5)
General disorders and administration site conditions	
Pyrexia	4/8 (50.0)
Injury, poisoning and procedural complications	
Pseudomeningocele	2/8 (25.0)
Fall	1/8 (12.5)
Stoma site irritation	1/8 (12.5)
Subdural hematoma	1/8 (12.5)
Skin and subcutaneous tissue disorders	
Rash	3/8 (37.5)
Scalp irritation	1/8 (12.5)
Skin reaction	1/8 (12.5)
Skin swelling	1/8 (12.5)
Blood and lymphatic system disorders	
Neutrophilia	1/8 (12.5)
Pancytopenia	1/8 (12.5)
Respiratory, thoracic and mediastinal disorders	
Nasal congestion	1/8 (12.5)
Other respiratory disorder	1/8 (12.5)
Eye disorders	
Chalazion, left eye	1/8 (12.5)
Investigations	
CSF white blood cell count increased	1/8 (12.5)
Electroencephalogram abnormal	1/8 (12.5)
Metabolism and nutrition disorders	
Malnutrition	1/8 (12.5)

1,000-fold concentration gradient (micromolar in CSF versus millimolar in the brain). Changes in NAA levels in CSF imply a correction of functional brain ASPA activity. We observed a fast decline in NAA concentration starting 1 month after treatment, and there was a continuous decline up to 24 months after treatment, suggesting sustained *ASPA* expression.

Magnetic resonance spectroscopy. NAA concentrations were also indirectly assessed using non-invasive single-voxel magnetic resonance spectroscopy (MRS) techniques. In the occipital region, which has the highest concentrations of NAA overall owing to a physiological rostral–caudal NAA gradient (our primary target area for assessments), the linear mixed-effects model showed a small, non-significant slope downward of −0.02 mM month^{-1} (Extended Data Fig. 1). On review of individual participant data, the 3 participants with 24-month follow-up data (001, 002, 003) showed a 2–3-mM drop in primarily white matter NAA at 24 months, which we prospectively proposed to be a clinically significant change. The three youngest participants with lower levels of NAA at baseline showed less relative change, with a flat or slightly increasing slope. Other brain regions were sampled, including frontal lobes and basal ganglia, but these were not included in primary analysis.

Synthetic magnetic resonance imaging. Because dysmyelination is the fundamental cause of the functional deficits associated with CD, any successful therapeutic intervention needs to increase myelination. To detect increases in myelination, we used a novel imaging technique, synthetic magnetic resonance imaging (SyMRI), to measure brain volumes specific to myelin and water content (Supplementary Methods). This magnetic resonance imaging toolkit permits a substantial decrease in scan time, useful for pediatric participants, along with fully quantitative analysis of imaging data with comparison to normative pediatric data[23]. Linear mixed-effects analysis of SyMRI myelin volume showed a statistically significant increase from baseline over time (Fig. 2). The population coefficient estimate was 0.706 ml month^{-1} with a standard error of 0.2623, $P = 0.0137$. Myelin changes for individual participants are shown in Extended Data Fig. 2. Compared with normal reference values, the values of all treated patients fall in the 95% confidence interval (CI) range of healthy 1-year-old children. Because CD is a rare disease and limited pretreatment data were available, no population reference values are available at this time specifically for CD, but previous natural history studies[24] suggested loss of brain mass and trivial gains in white matter beyond 12 months of age.

For assessment of developmental milestones with respect to age and time from treatment, we used clinical metrics for which reference values were obtained in our previous rAAV vector-based clinical study for CD[17]: the Mullen Scales of Early Learning (MSEL) and GMFM-88. The MSEL is a standardized instrument designed to assess language, motor and perceptual abilities in children from birth to 68 months of age. GMFM-88 is a standardized instrument that was originally designed and validated to measure gross motor function in patients with cerebral palsy by assessing physical abilities from lying and rolling to walking, jumping and running.

MSEL. For our primary analysis of clinical data, we used multivariate mixed-model regression to compare posttreatment MSEL scores of treated FIH study participants versus benchmark data consisting of pretreatment FIH study participants and untreated NH patients. The NH control data were from ten untreated patients for whom historical data were available. These patients were aged 3–60 months at the time of data collection (that is, within the age window for eligibility for this study) with multiple longitudinal data points available. The treated (FIH) and untreated (NH) groups did not differ significantly in baseline features including genetic mutations, age and sex (Extended Data Table 1).

https://doi.org/10.1038/s41591-025-03919-w

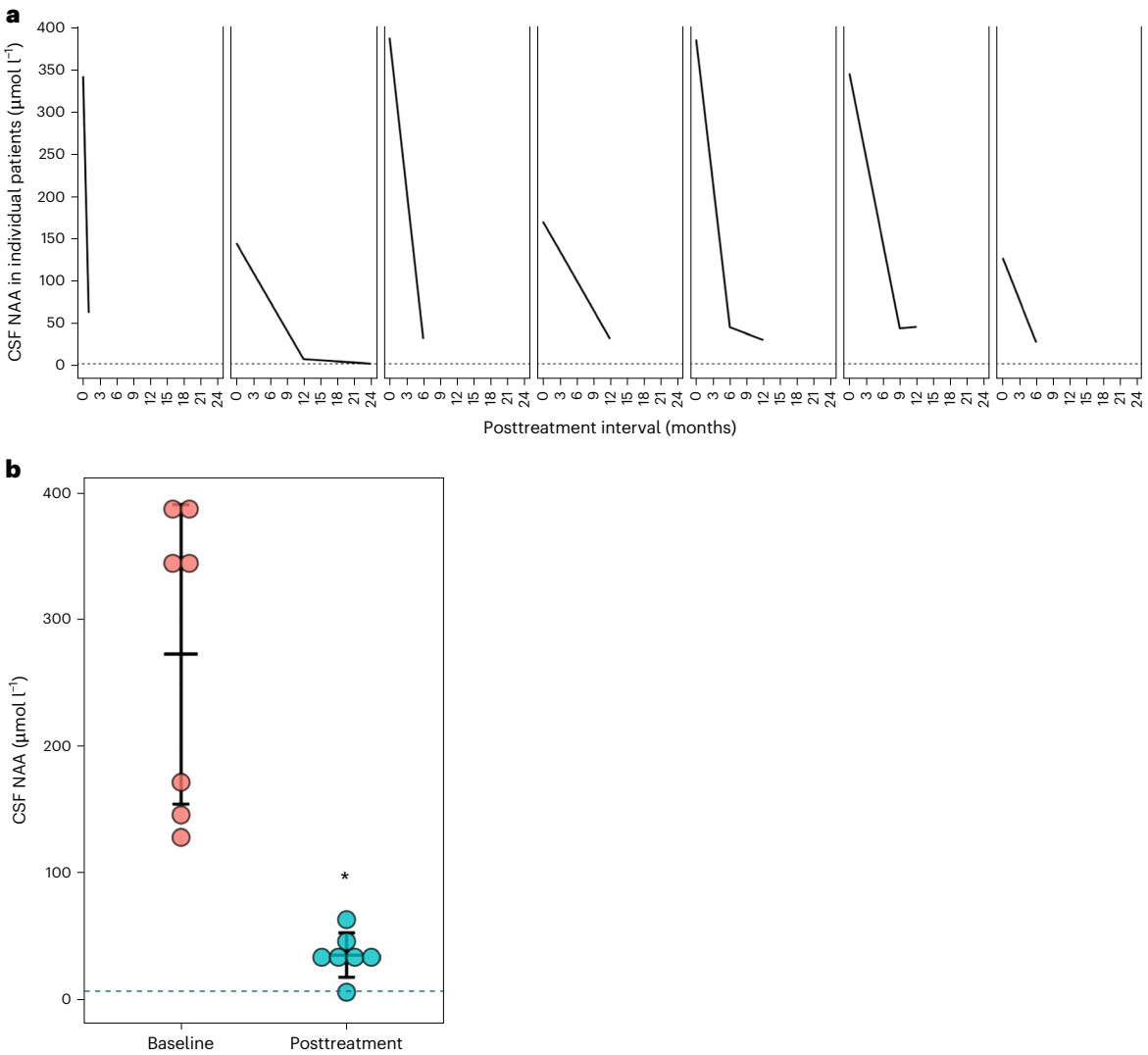

Fig. 1 | Change in NAA concentration in CSF after MYR-101 treatment. **a**, Change in CSF NAA concentrations following treatment, showing a decrease from baseline in every participant measured. One participant's family refused CSF collection after treatment. Data for the other seven participants are shown. The dotted line shows the upper bound of normal NAA concentration in CSF of approximately 3 µM. **b**, NAA concentrations in CSF at baseline and after treatment ($n = 7$). The center bar indicates the median; the bottom and top bars indicate 5% and 95% percentiles, respectively. The dotted line shows the upper bound of normal CSF values, approximately 3 M.

For comparison of the overall treatment effect across all five MSEL domains between the treated and untreated groups, a multivariate mixed-model repeated-measures (MMRM) approach was used for analysis of MSEL raw scores and MSEL developmental age. We detected a statistically significant improvement in MSEL scores of participants following MYR-101 treatment compared with historic reference scores of untreated CD controls. The overall treatment effect across all five MSEL domain raw scores was significantly different controlling for baseline chronological age between the two groups ($P = 0.0171$). The result for MSEL developmental age was similar to that observed for MSEL raw scores. Multivariate MMRM analysis showed that the overall treatment effect across all MSEL domain developmental ages was significantly different, controlling for baseline chronological age, between the treated and untreated groups for raw scores ($P = 0.0253$) (Fig. 3a).

While the multivariate MMRM analysis offered a comprehensive view of the overall impact across multiple domains, the univariate MMRM analysis made it possible to isolate and interpret the treatment effects on each specific MSEL domain. This approach clarified the contributions of each domain to the overall treatment effect, identified any domain-specific responses or variations and provided a more granular understanding of how the therapy impacts different aspects of development in CD. For the receptive language domain (Fig. 3b), results of univariate MMRM analysis showed that the rate of increase between the treated and untreated groups in receptive language scores was significantly different controlling for baseline chronological age (treatment-by-time interaction = 0.35; 95% CI = 0.047, 0.651; $P = 0.0261$). This indicates that the rate of increase in the receptive language raw score in the treated group was significantly higher than in the untreated group. For the visual reception domain (Fig. 3c), the rate of increase was significantly different between the treated and untreated groups in the visual reception raw score controlling for baseline chronological age (treatment-by-time interaction = 0.57; 95% CI = 0.126, 1.008; $P = 0.0145$). This indicates that the treated group had a significantly higher rate of increase over time in the visual reception raw score compared with the untreated group. For the fine motor domain (Fig. 3d), there was a trend for improvement ($P = 0.0541$). No significant differences in the rate of change between treated and untreated groups were observed for the gross motor MSEL raw score ($P = 0.4816$) (Fig. 3e) or the expressive language MSEL raw score ($P = 0.5031$) (Fig. 3f) based on the univariate MMRM analyses.

https://doi.org/10.1038/s41591-025-03919-w

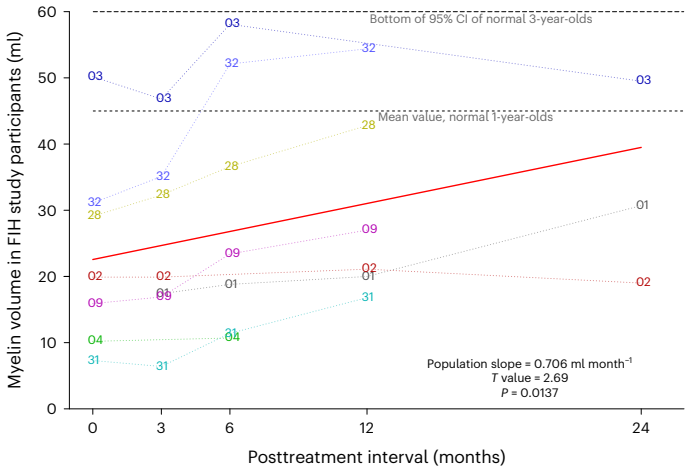

Fig. 2 | Change in total brain myelin volumes after MYR-101 treatment. Mean change in whole-brain myelin volume for individual participants, measured by SyMRI. Population fit (that is, mean volume with respect to time from treatment) for the study population is shown by the solid red line. Myelin content was analyzed using a two-sided *t*-test and showed statistically significant change and positive slope compared with the baseline at both 6 months ($P = 0.04$) and 12 months ($P = 0.03$), measured with the paired *t*-statistic. The population slope from the linear mixed-effects model was positive and significantly different from zero ($T = 2.69$, $P = 0.0137$). For reference, the mean myelin content for normal 1-year-olds is shown by the lower horizontal dashed line, and the lower limit of 95% CI myelin content for normal 3-year-olds is shown by the upper horizontal dashed line. On the basis of previously published reference data[24], the 95% CI for myelin content of normal 1-year-olds is 10–70 ml; the total myelin of all treated participants with CD fell into this range. Because participants were not followed for an extended period before treatment, there is no population fit for myelin content in untreated participants with CD, but our previous natural history studies showed monotonically decreasing myelin and white matter volumes with age[25].

Gross motor function measure. The GMFM-88 also was used to independently assess motor abilities. Most patients with CD score in the first two domains only: lying and rolling and sitting domain. Raw scores for these GMFM-88 domains are shown in Extended Data Fig. 3. The posttreatment population slope in the GMFM-88 lying and rolling domain, estimated by linear mixed-effects modeling, was 0.208 points per month ($P = 0.2623$). In the GMFM-88 sitting domain, the posttreatment population slope was estimated to be slightly lower at 0.157 points per month ($P = 0.4114$). We anticipate stronger results when a longer follow-up period is available. Only one participant showed any score on the kneeling and crawling domain. Representative patient outcomes are shown visually in video clips (Supplementary Video 1).

Discussion

This planned interim analysis showed that MYR-101 is well tolerated at the current dose of 3.7×10^{13} vector genomes (vg), showing positive target engagement, with statistically significant improvements in clinical scores and key biomarkers. The study's strengths include rigorous inclusion criteria, excluding participants with atypical and mild CD, and the use of validated clinical outcome measures. Participant safety was prioritized through the inclusion of waiting periods between the treatments of the first three participants. Despite the requirement for a neurosurgical procedure, intracerebroventricular (ICV) administration of MYR-101 was advantageous because direct brain delivery allowed the use of a lower dose of gene therapy vector compared with systemic administration and can be expected to minimize systemic immunological side effects.

Our choice of vector route was supported by preclinical studies confirming MYR-101 biodistribution and transgene expression in an animal model[18]. Over two decades ago, our gene therapy study with AAV2 for CD[17] used direct intraparenchymal brain delivery to avoid issues related to limited blood–brain barrier penetration; that study targeted neurons with a goal of lowering global NAA concentrations and showed a statistically significant 2–3-mM drop in NAA levels in a variety of brain areas assessed by MRS, but without sustained clinical improvement. In this new study targeting oligodendrocytes, we adapted our original delivery approach using a hybrid intracerebral delivery paradigm with catheter-based delivery to the cerebral ventricle.

In addition to our own preclinical studies, a variety of studies by other investigators have shown variable efficacy of vector distribution using different AAV vectors for inherited neurometabolic diseases, when delivered via intracisternal, ICV, intrathecal, intravenous and other routes, and at different doses[25,26]. Debate continues on which delivery route is optimal, and the answer may be disease and vector dependent. Recently, a variety of other gene therapy clinical trials have targeted a variety of brain diseases using ICV delivery, including Rett syndrome (https://clinicaltrials.gov/study/NCT05898620), Batten disease (https://clinicaltrials.gov/study/NCT05228145), Dravet's syndrome (https://clinicaltrials.gov/study/NCT05419492) and NGLY1 deficiency (https://clinicaltrials.gov/study/NCT06199531).

There is currently another ongoing clinical trial for CD using rAAV9 gene therapy (NCT04998396), differing in vector design and targeting strategy. The selective tropism of MYR-101 for oligodendrocytes directly addresses the core pathology of dysmyelination. Although there is some theoretical concern that late-stage CD in humans may manifest with destruction of oligodendroglia to the extent that remaining cells may not express sufficient ASPA to counteract the disease course, our results to date do not support that concern. In fact, encouragingly, older patients also show measurable progress and detectable changes in multiple outcome measures. In terms of clinical outcomes, improvements were observed across all five MSEL domains and the aggregate developmental score. Gains in gross motor function (for example, head lag, mobility) and expressive language were of lower magnitude and not statistically significant, and GMFM-88 scores showed limited improvements. Improvements were observed in the GMFM-88 lying and rolling domain and sitting domain, but changes did not reach statistical significance. Long-term monitoring in the full study cohort may elucidate whether GMFM-88 score improvements in MYR-101-treated participants continue over time and whether they reach significance.

Biomarker analysis included myelin volume assessed with SyMRI, along with NAA concentrations measured in CSF and by MRS. While untreated patients with CD typically show progressive brain atrophy and myelin loss over time, we observed significant increases in myelin volume after MYR-101 administration (Figs. 2 and 4). These improvements exceeded the limited increases noted in our previous clinical study[17,24]. Increased myelination in CD treatment is a crucial finding because myelin loss is a hallmark of the disease, and its restoration is a major improvement from the expected natural history. Such a degree of myelination improvement has not been previously documented in the literature for CD, in which the typical clinical course is characterized by progressive myelin loss. Reduction in extraparenchymal water content (EPW) was also observed along with myelin increase, suggesting brain water shifts that are consistent with our knowledge of osmotic dysregulation in CD.

NAA concentrations showed a statistically significant reduction in CSF. Reduction in NAA concentration is a key indicator of therapeutic efficacy in CD, but its compartmentalization in the brain complicates interpretation. While elevated NAA concentration in the interstitial fluid and CSF is pathological, precipitous drops in parenchymal NAA concentration as measured with MRS are not necessarily expected or desirable and could indicate neuronal damage rather than correction in target cells in white matter. Further testing of interstitial NAA in

https://doi.org/10.1038/s41591-025-03919-w

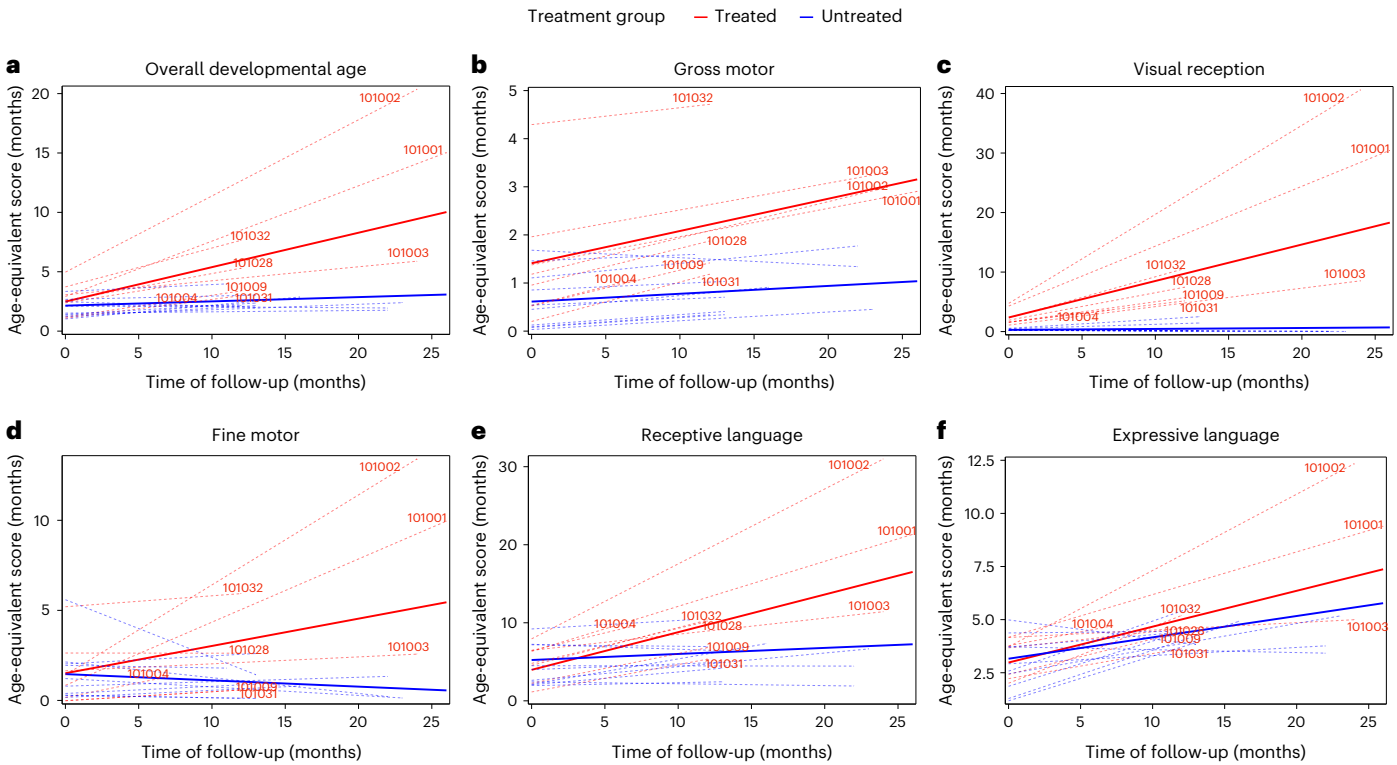

Fig. 3 | MSEL aggregate developmental score and subdomains. Panels showing MMRM regression lines for MSEL for treated patients (red dashed lines) and an age-matched reference group of untreated patients with CD (blue dashed lines). **a**–**f**, Results for overall developmental age (**a**), gross motor skills (**b**), visual reception (**c**), fine motor skills (**d**), receptive language (**e**) and expressive language (**f**). The solid lines denote the mean population lines, red for the treated group and blue for the untreated reference group. Plots show developmental age equivalents as a function of time from treatment (or age-matched reference), using normative data scales from the MSEL reference manual. Raw scores were converted to developmental means based on the reference tables within the MSEL manual. The MSEL overall developmental age represents the five-domain arithmetic mean MSEL developmental age.

experimental models with in vivo microdialysis may help to answer this important question about the partitioning of NAA during the disease process.

Direct CSF analysis with HPLC is highly sensitive and specific for detecting NAA concentrations, providing an accurate quantitative assessment. By contrast, MRS offers a semiquantitative measurement of NAA, which is dependent on assumptions of white versus gray matter composition and voxel selection. It should be noted that brain solute concentrations measured by MRS are volume averaged over both gray and white matter regions, and voxel selection can contribute to some variability in measurements owing to shimming effects. Single-voxel MRS may miss localized changes, especially in regions affected by partial volume effects or when changes are diffuse rather than focal. The NAA concentration gradient from the brain to CSF is typically over three orders of magnitude, with NAA concentrations in normal pediatric CSF ranging from 0.25 µM to 3 µM (ref. 27) and NAA concentrations in CD CSF typically ranging from 400 µM to 900 µM (ref. 28), so CSF values are an indirect measure of NAA changes in the brain and interstitial fluid. Data from the full study cohort may shed further light on this.

It should be noted that in the four older participants (001, 002, 003, 004), we observed a 2–3-mM-magnitude drop of white matter NAA (Extended Data Fig. 1) as measured with MRS over 0–24 months (1 participant lost to follow-up), together with a statistically significant drop in NAA directly in CSF. Participants 009, 028, 031 and 032 were younger and had lower NAA values at baseline. Interestingly, these participants showed less relative change in white matter NAA as measured by MRS over 12 months, compared with the older, more severely affected participants, but showed a similar large relative drop in CSF levels of NAA.

The overall safety of MYR-101 gene therapy was consistent with other studies of intracerebral gene therapy administration[17,29]. In terms of safety, we captured and reviewed AEs based on their relatedness to either the MYR-101 drug product or the neurosurgical procedure. Because MYR-101 administration cannot be separated from the neurosurgical procedure, distinguishing between these causes was crucial. Two versions of the neurosurgical procedure were used during the study. In the first three participants, MYR-101 was administered via four ICV injections using a peel-away sheath. After these initial procedures, the protocol was modified to reduce the number of injection sites to two (one in each lateral ventricle of the brain) and to abandon the peel-away sheath in favor of a guide wire for catheter placement.

Most SAEs related to the neurosurgical procedure occurred in the first three participants. These included a CSF leak and two seizure episodes. Non-serious pseudomeningocele events occurred in two participants. Following the procedural change, no SAEs related to the neurosurgical procedure were reported. The only mild AE related to the procedure afterward was scalp edema in one participant. All AEs and SAEs resolved fully, with participants making complete recoveries. No SAEs were attributed to the MYR-101 drug product itself. The only non-SAEs possibly related to MYR-101 were moderate fever and mild rash in one participant, both of which resolved quickly with antipyretic medication.

Among the AEs observed, seizures warrant particular attention owing to their frequency in CD and their potential association with both the underlying pathology and the neurosurgical procedure. Seizures occur in approximately 60% of patients with CD, with onset around 9.5 months of age, and affect nearly all patients by 10 years of age[12,30]. The neurodegenerative nature of the disease inherently increases seizure risk due to progressive brain dysfunction. In the context of our

https://doi.org/10.1038/s41591-025-03919-w

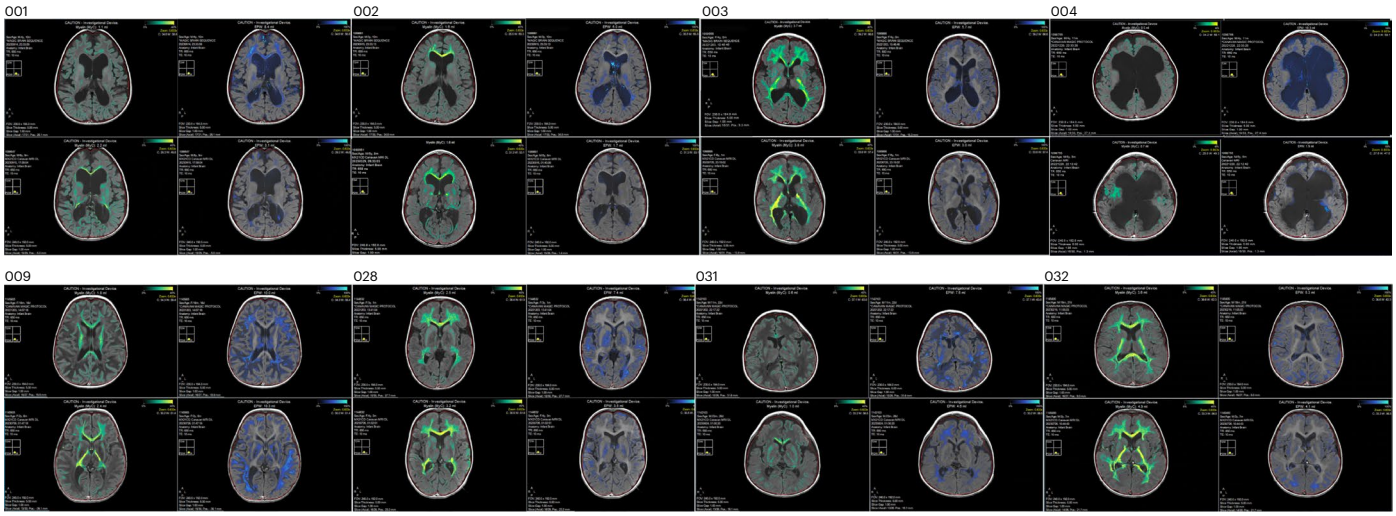

Fig. 4 | Baseline and posttreatment brain myelin and water content in MYR-101-treated participants. This is a panoramic view of the eight treated participants, showing a representative slice through large white matter tracts including the corpus callosum and internal capsule. Each participant's baseline is at the top, and the posttreatment interval is shown at the bottom. Color-enhanced images for each participant show myelin content at the left (green) and EPW at the right (blue) as calculated by SyMRI. The myelination and EPW (brain edema) are proportional to the color intensity and are obvious upon inspection. In 8 out of 8 participants, the myelin content of this white matter-containing brain region increased or was relatively unchanged, and interstitial water content decreased in 7 out of 8 participants, consistent with *ASPA* expression in oligodendrocytes and more myelin being generated. We observed a consistent inverse relationship between myelin content and EPW, consistent with the known pathophysiology of CD, in which myelin becomes water logged and degenerates with time. In these images, it is evident that increased myelin generally occurred in concert with a decrease in EPW. In addition to the visual display of myelin content in these representative slices, whole-brain myelin and water content are shown in Extended Data Table 2, with an increase or relative stabilization in all participants. Follow-up periods are 24 months for participants 001, 002 and 003; 6 months for participant 004; and 12 months for participants 009, 028, 031 and 032. The mean myelin increase was 135%, with a corresponding mean EPW decrease of 26%. In this group, 7 out of 8 participants showed a decrease in EPW, 6 out of 8 showed a substantial increase in myelin (>100% change) and the other 2 out of 8 showed relatively stable myelination (≤4% change) over time. The youngest participants and those with less myelin at baseline showed the largest relative increases, while those with the highest levels of myelin at baseline showed smaller relative increases. These data are consistent with Fig. 2 showing total brain myelin content versus the baseline for all patients, with a statistically significant increase in mean total brain myelin content from baseline. It is evident from Extended Data Table 2 that patients who were older at baseline and in whom a rigid peel-away guide catheter was used (001, 002, 003) showed relatively less increase in myelin, compared with the other patients.

study, seizures are classified as AEs of special interest owing to their potential severity and impact on clinical outcomes. Seizures may arise from the disease itself or as a consequence of treatment. Although seizures are not commonly reported after external ventricular drain placement[31] (a procedure similar in nature to our ICV injections), the invasive nature of neurosurgical procedures can precipitate seizures. Contributing factors may include direct mechanical irritation from the catheter, hemorrhagic complications, infections or the underlying brain pathology.

Limitations of the study should be considered in interpreting our results. Long-term outcomes and the durability of treatment effect are yet to be fully assessed, requiring ongoing follow-up in the full study cohort. In addition, discrepancies between NAA concentrations in CSF and brain tissue (via MRS) underscore the need for further investigation into NAA compartmentalization. Although ICV delivery is believed to optimize vector targeting, changes in the procedure, such as were already done after treatment of the first three participants, could enhance feasibility and accessibility of the therapy. Finally, mild atypical cases of CD were deliberately excluded, with strict inclusion criteria focusing on typical CD with severely affected patients at baseline. Thus, the effect in less severely affected patients is unknown.

In summary, this interim analysis showed that MYR-101 is well tolerated and shows preliminary evidence of efficacy, including statistically significant reductions in CSF NAA concentrations, statistically significant increases in myelin volumes and clinical improvement in MSEL compared with an NH cohort. AEs were mostly related to the neurosurgical procedure, and modifications to the surgical protocol improved safety outcomes. Continued monitoring of these events and long-term follow-up will be critical to understanding the full therapeutic potential of MYR-101. These findings represent an important step toward developing a disease-modifying therapy for CD and may provide a foundation for treating other demyelinating and metabolic brain disorders.

Online content

Any methods, additional references, Nature Portfolio reporting summaries, source data, extended data, supplementary information, acknowledgements, peer review information; details of author contributions and competing interests; and statements of data and code availability are available at https://doi.org/10.1038/s41591-025-03919-w.

References

1. Canavan, M. M. Schilder's encephalitis periaxialis diffusa: report of a case of a child aged sixteen and one-half months. *Arch. Neurol. Psychiatry* **25**, 299–308 (1931).
2. Leone, P. et al. Aspartoacylase gene transfer to the mammalian central nervous system with therapeutic implications for Canavan disease. *Ann. Neurol.* **48**, 27–38 (2000).
3. Matalon, R., Kaul, R. & Michals, K. Canavan disease: biochemical and molecular studies. *J. Inherit. Metab. Dis.* **16**, 744–752 (1993).
4. Baslow, M. H. Canavan's spongiform leukodystrophy: a clinical anatomy of a genetic metabolic CNS disease. *J. Mol. Neurosci.* **15**, 61–69 (2000).
5. Francis, J. S. et al. *N*-Acetylaspartate supports the energetic demands of developmental myelination via oligodendroglial aspartoacylase. *Neurobiol. Dis.* **96**, 323–334 (2016).
6. Hoshino, H. & Kubota, M. Canavan disease: clinical features and recent advances in research. *Pediatr. Int.* **56**, 477–483 (2014).

7. Lotun, A., Gessler, D. J. & Gao, G. Canavan disease as a model for gene therapy-mediated myelin repair. *Front. Cell. Neurosci.* **15**, 661928 (2021).
8. Janson, C. G. et al. Mild-onset presentation of Canavan's disease associated with novel G212A point mutation in aspartoacylase gene. *Ann. Neurol.* **59**, 428–431 (2006).
9. Velinov, M., Zellers, N., Styles, J. & Wisniewski, K. Homozygosity for mutation G212A of the gene for aspartoacylase is associated with atypical form of Canavan's disease. *Clin. Genet.* **73**, 288–289 (2008).
10. Adachi, M., Schneck, L., Cara, J. & Volk, B. W. Spongy degeneration of the central nervous system (van Bogaert and Bertrand type; Canavan's disease). A review. *Hum. Pathol.* **4**, 331–347 (1973).
11. Matalon, R. et al. Aspartoacylase deficiency and *N*-acetylaspartic aciduria in patients with Canavan disease. *Am. J. Med. Genet.* **29**, 463–471 (1988).
12. Traeger, E. C. & Rapin, I. The clinical course of Canavan disease. *Pediatr. Neurol.* **18**, 207–212 (1998).
13. Bokhari, M. R., Samanta, D. & Bokhari, S. R. A. *Canavan Disease* (StatPearls Publishing, 2024).
14. Zelnik, N. et al. Protracted clinical course for patients with Canavan disease. *Dev. Med Child Neurol.* **35**, 355–358 (1993).
15. Zeng, B. J. et al. Identification and characterization of novel mutations of the aspartoacylase gene in non-Jewish patients with Canavan disease. *J. Inherit. Metab. Dis.* **25**, 557–570 (2002).
16. Janson, C. et al. Clinical protocol. Gene therapy of Canavan disease: AAV-2 vector for neurosurgical delivery of aspartoacylase gene (*ASPA*) to the human brain. *Hum. Gene Ther.* **13**, 1391–1412 (2002).
17. Leone, P. et al. Long-term follow-up after gene therapy for Canavan disease. *Sci. Transl. Med.* **4**, 165ra3 (2012).
18. Francis, J. S. et al. Preclinical biodistribution, tropism, and efficacy of oligotropic AAV/Olig001 in a mouse model of congenital white matter disease. *Mol. Ther. Methods Clin. Dev.* **20**, 520–534 (2021).
19. Traka, M. et al. *Nur7* is a nonsense mutation in the mouse aspartoacylase gene that causes spongy degeneration of the CNS. *J. Neurosci.* **28**, 11537–11549 (2008).
20. Hull, V. et al. Antisense oligonucleotide reverses leukodystrophy in Canavan disease mice. *Ann. Neurol.* **87**, 480–485 (2020).
21. Maier, H., Wang-Eckhardt, L., Hartmann, D., Gieselmann, V. & Eckhardt, M. *N*-Acetylaspartate synthase deficiency corrects the myelin phenotype in a Canavan disease mouse model but does not affect survival time. *J. Neurosci.* **35**, 14501–14516 (2015).
22. Pleasure, D. et al. Pathophysiology and treatment of Canavan disease. *Neurochem. Res.* **45**, 561–565 (2020).
23. McAllister, A. et al. Quantitative synthetic MRI in children: normative intracranial tissue segmentation values during development. *Am. J. Neuroradiol.* **38**, 2364–2372 (2017).
24. Janson, C. G. et al. Natural history of Canavan disease revealed by proton magnetic resonance spectroscopy (1H-MRS) and diffusion-weighted MRI. *Neuropediatrics* **37**, 209–221 (2006).
25. Mendell, J. R. et al. Single-dose gene-replacement therapy for spinal muscular atrophy. *N. Eng. J. Med.* **377**, 1713–1722 (2017).
26. Whitley, C. B. et al. Final results of the phase 1/2, open-label clinical study of intravenous recombinant human *N*-acetyl-α-d-glucosaminidase (SBC-103) in children with mucopolysaccharidosis IIIB. *Mol. Genet. Metab.* **126**, 131–138 (2019).
27. Jakobs, C. et al. Stable isotope dilution analysis of *N*-acetylaspartic acid in CSF, blood, urine and amniotic fluid: accurate postnatal diagnosis and the potential for prenatal diagnosis of Canavan disease. *J. Inherit. Metab. Dis.* **14**, 653–660 (1991).
28. Kolodziejczyk, K., Hamilton, N. B., Wade, A., Káradóttir, R. & Attwell, D. The effect of *N*-acetyl-aspartyl-glutamate and *N*-acetyl-aspartate on white matter oligodendrocytes. *Brain* **132**, 1496–1508 (2009).
29. Corti, M. et al. Adeno-associated virus-mediated gene therapy in a patient with Canavan disease using dual routes of administration and immune modulation. *Mol. Ther. Methods Clin. Dev.* **30**, 303–314 (2023).
30. Bley, A. et al. The natural history of Canavan disease: 23 new cases and comparison with patients from literature. *Orphanet J. Rare Dis.* **16**, 227 (2021).
31. Janson, C. G., Romanova, L. G., Rudser, K. D. & Haines, S. J. Improvement in clinical outcomes following optimal targeting of brain ventricular catheters with intraoperative imaging. *J. Neurosurg.* **120**, 684–696 (2014).

[1]Rowan-Virtua Health College of Medicine and Life Sciences, Rowan-Virtua SOM and Translational Biomedical Engineering and Sciences, Stratford, NJ, USA. [2]Wright State-Premier Health Neuroscience Institute, Dayton, OH, USA. [3]Division of Neurosurgery, Dayton Children's Hospital, Dayton, OH, USA. [4]Myrtelle, Inc., New York, NY, USA. [5]Departments of Radiology, Pediatrics, Neuroscience, Environmental and Public Health Sciences, University of Cincinnati College of Medicine, Cincinnati, OH, USA. [6]These authors contributed equally: Paola Leone, Robert M. Lober. ✉e-mail: OFlamini@MyrtelleGTX.com; janson@memorymatters.org

Methods

This phase 1/2 FIH study (NCT04833907) was designed to obtain safety and efficacy data following neurosurgical administration of a single dose of MYR-101, delivered via four ICV injection sites in the first three participants and two ICV injection sites in subsequent participants with CD. To ensure consistency of procedures and dose administration, the study was conducted at a single site, Dayton Children's Hospital. The primary objective of the study was to assess the safety and tolerability of ICV dosing of MYR-101 in children with typical CD. Primary safety endpoints were AEs, routine laboratory tests and absence of inflammation or other acute intracranial pathology on magnetic resonance imaging. Efficacy of intracranial dosing with MYR-101 was assessed with standardized clinical testing with the MSEL and GMFM-88; analysis of NAA concentration with direct sampling of CSF for quantification by mass spectrometry as well as non-invasive MRS in selected brain regions using LCModel with phantom standardization; and volumetric analysis of myelination, white matter and extracellular water content by quantitative SyMRI. Per protocol, participants are assessed at baseline and at 1, 3, 6, 12, 24, 36, 48 and 60 months after the procedure for safety and efficacy. Principal investigators were responsible for participant screening and confirmation of study eligibility. All participants underwent pre-enrollment screening that included genotyping and definitive diagnosis of typical CD by a board-certified neurologist. After meeting all study enrollment criteria (Supplementary Methods), participants were selected for treatment in order of enrollment from among three age-based treatment cohorts.

Reporting summary

Further information on research design is available in the Nature Portfolio Reporting Summary linked to this article.

Data availability

At the outset of the trial, we omitted a data-sharing provision from the consent documents signed by participants. As a result, in accordance with our Ethics Committee policies, we are not authorized to release the raw data to the public. Furthermore, the study is still in progress. De-identified patient characteristics, safety and preliminary efficacy data from raw datasets generated in this study are included in the paper. Requests for more information about the raw data are subject to a confidentiality agreement with Myrtelle and must comply with applicable legal and regulatory requirements. Qualified researchers may request access to the trial information by contacting corresponding author O.F. The requests will be addressed within 120 days, and data transfer agreement may be required.

Acknowledgements

We thank the patients and families who generously contributed their time, courage and commitment to this research that made this study possible. We also wish to thank all of the Canavan Disease Patient Advocacy Groups worldwide for their commitment to research and patient care in this community, and the entire team at Dayton Children's Hospital for their support and collaboration. We sincerely thank S. Hesterlee, now interim president and CEO of the Muscular Dystrophy Association, for her exceptional guidance and support during the early development of this program in her former role as program director of the Canavan Disease Program. We also thank L. E. Kratz and the Kennedy Krieger Institute Biochemical Genetics Lab for analyzing the CSF NAA samples. We thank A. Pace for statistical support on this project, particularly with MSEL statistical analysis. We also wish to acknowledge the important scientific contributions of J. R. Samulski and S. Gray, whose expertise has been instrumental during the first phase of this program. We gratefully acknowledge the members of the Independent Data Monitoring Committee for their expert guidance, oversight and commitment to ensuring the integrity of the trial. Their independent review and thoughtful recommendations have been invaluable in guiding the conduct of this study. We thank the FDA for their supportive guidance and for recognizing the urgent, unmet needs of patients and families affected by this devastating disease and their commitment to accelerating the progress of this program. This study is funded by Myrtelle, Inc. Paper preparation support, provided by J. G. Jacobson, InSeption Group, was also funded by Myrtelle, Inc.

Author contributions

P.L. contributed to study design, data interpretation, revision of the paper and approval of the paper for submission. R.M.L. contributed to data interpretation, revision of the paper and approval of the paper for submission. J.F. contributed to data interpretation, revision of the paper and approval of the paper for submission. O.F. contributed to data interpretation, writing and revision of the paper and approval of the paper for submission. C.G.J. contributed to data analysis and interpretation, writing and revision of the paper, approval of the paper for submission. D.S. contributed to statistical analyses, revision of the paper and approval of the paper for submission. K.M.C. contributed to data interpretation, revision of the paper and approval of the paper for submission.

Competing interests

P.L. is a shareholder of and paid consultant for Myrtelle, Inc. R.M.L. and J.F. report no conflicts of interest. C.G.J., D.S. and K.M.C. are paid consultants for Myrtelle, Inc. O.F. is co-chief medical officer and a shareholder of Myrtelle, Inc.

Additional information

Extended data is available for this paper at https://doi.org/10.1038/s41591-025-03919-w.

Supplementary information The online version contains supplementary material available at https://doi.org/10.1038/s41591-025-03919-w.

Correspondence and requests for materials should be addressed to Olga Flamini or Christopher G. Janson.

Peer review information *Nature Medicine* thanks Evan Snyder and the other, anonymous, reviewer(s) for their contribution to the peer review of this work. Primary Handling Editor: Jerome Staal in collaboration with the *Nature Medicine* team.

https://doi.org/10.1038/s41591-025-03919-w

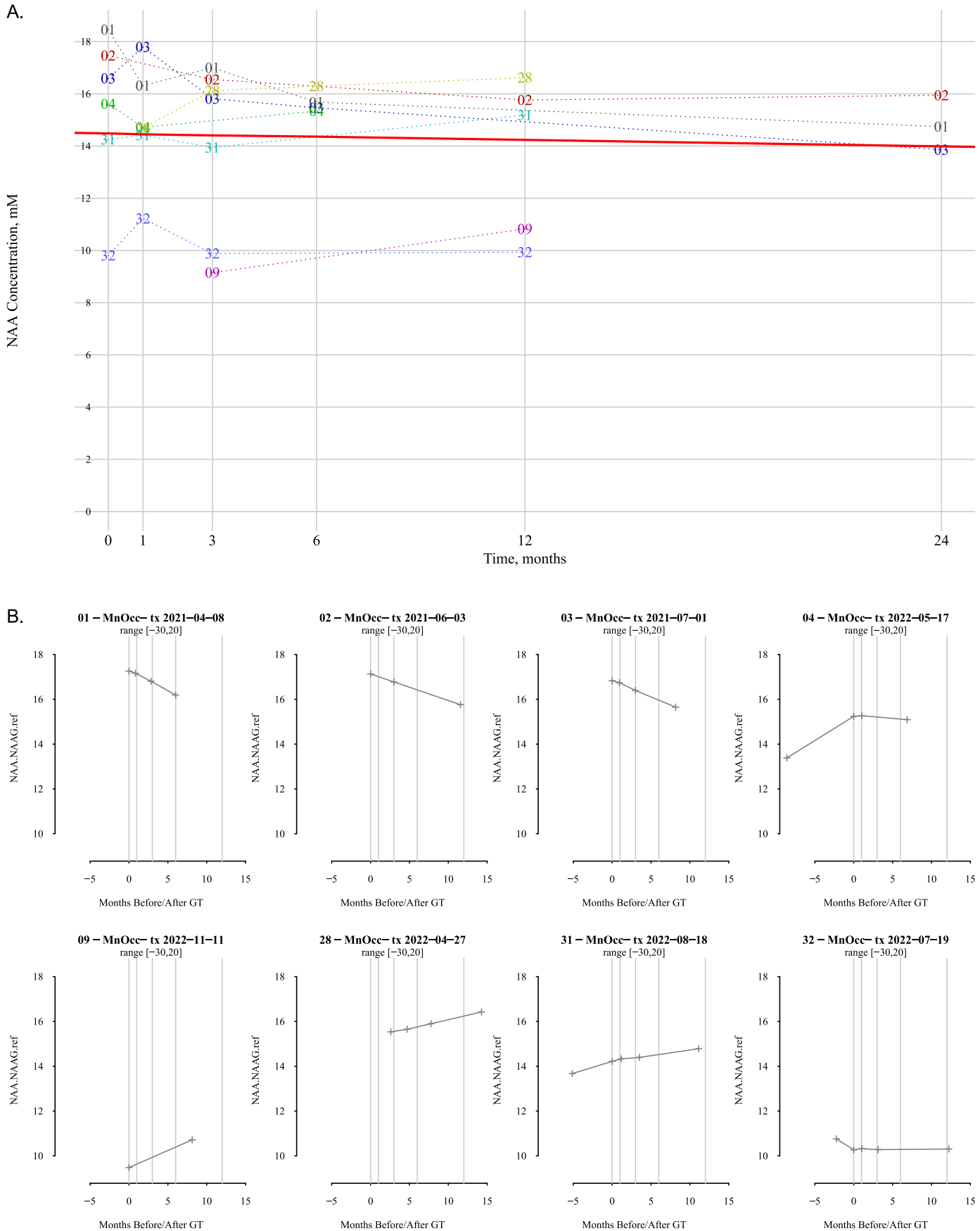

Extended Data Fig. 1 | See next page for caption.

https://doi.org/10.1038/s41591-025-03919-w

Extended Data Fig. 1 | Change in N-acetyl-aspartic acid (NAA) concentrations in the brain, measured by magnetic resonance spectroscopy after MYR-101 treatment. Panel a. Mean change in NAA across the occipital region for individual participants (average of right and left occipital voxels), measured by MRS. Population fit (i.e., mean line for the entire population) is shown in red. For reference, normal age-matched NAA concentrations in the occipital lobe range from 4-7 mM. **Panel b**. individual NAA values for each participant, including participant for whom pre-treatment values were available; in those participants, NAA slope was positive leading up to gene therapy and negative afterwards, as previously described[2].

https://doi.org/10.1038/s41591-025-03919-w

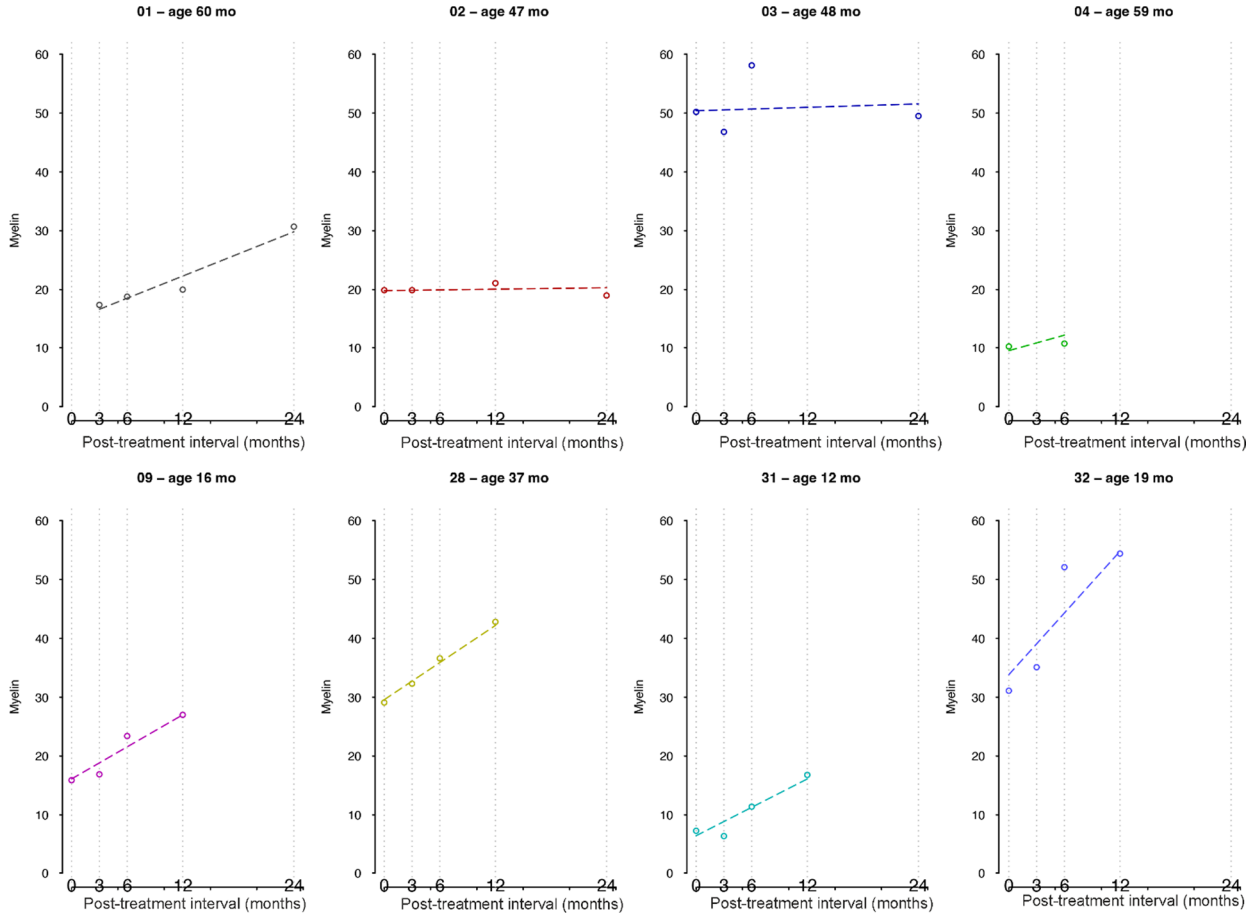

Extended Data Fig. 2 | Participant-level changes in myelin as a function of time from treatment. Myelin volume is shown in mLs. Participants are identified by their age at time of treatment.

https://doi.org/10.1038/s41591-025-03919-w

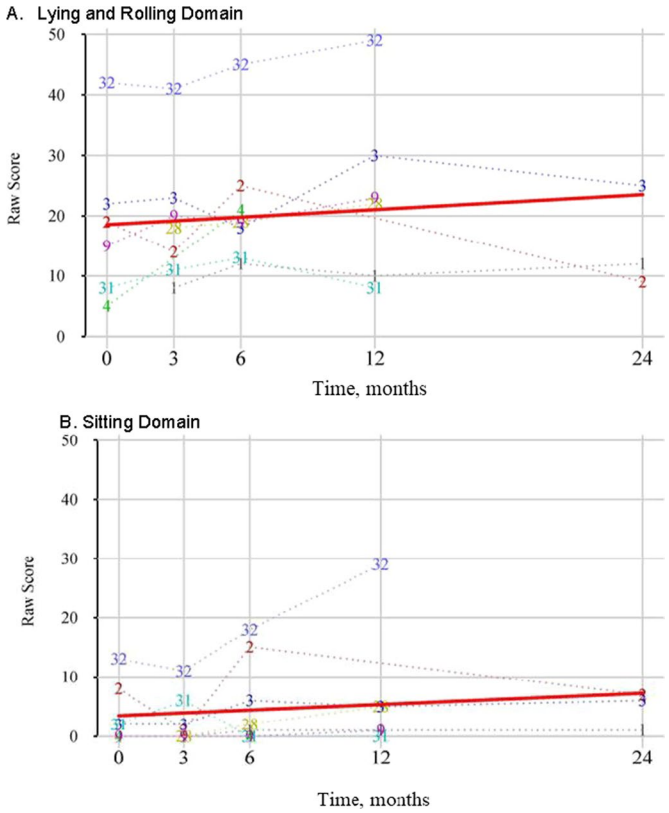

Extended Data Fig. 3 | Change in Gross Motor Function Measure (GMFM-88) raw scores in treated participants by chronological age. Panel a: Change in individual participants on the Lying and Rolling domain of the Gross Motor Function Measure. Population fit (mean line for the entire population) is shown in red. Panel b: Change in individual participants on the Sitting domain of the Gross Motor Function Measure. Population fit is shown in red.

https://doi.org/10.1038/s41591-025-03919-w

Extended Data Table 1 | Demographic data for patients in natural history database

Patient ID	Age (Months) at First MSEL Assessment	Sex	Country of Origin	*ASPA* Mutations
NH-001	39	F	Russia	854A>C 854A>C
NH-007	12	M	USA	548C>A unidentified deletion
NH-008	13	F	USA	914C>A 640G>T
NH-013	5	M	Germany	914C>A 362A>T
NH-024	47	M	USA	914C>A 550C>T
NH-025	44	F	USA	854A>C 854A>C
NH-027	11	F	Germany	859G>A unidentified
NH-028	7	F	USA	IVS 1-2A unidentified
NH-029	23	M	Great Britain	914C>A 914C>A
NH-031	7	M	Germany	914C>A 914C>A

Demographics of benchmark natural history data include genetic mutations, balanced male/female sex ratios, and other characteristics similar to the FIH participants. Abbreviations: *ASPA*, aspartoacylase gene; F, female; FIH, first-in-human participants; M, male; MSEL, Mullen Scales of Early Learning; NH, natural history patients; USA, United States of America.

https://doi.org/10.1038/s41591-025-03919-w

Extended Data Table 2 | Baseline and Post-treatment Brain Myelin and Water Content in MYR-101-Treated Participants

Subject ID	Age at treatment (months)	Interval (months)	Total brain myelin at baseline (mL)	Total brain myelin at interval (mL)	**% change myelin**	EPW at baseline (mL)	EPW at interval (mL)	**% change EPW**
001	57	24	17.5	30.7	+175%	123.0	54.1	-56.0%
002	47	24	19.8	19.0	-4.0%	82.5	30.3	-63.2%
003	48	24	50.3	49.7	-1.1%	90.1	53.4	-40.7%
004	59	6	7.2	10.9	+151%	155.5	37.5	-75.8%
009	18	12	16.0	27.0	+168%	132.4	163.3	+123 %
028	39	12	29.3	42.8	+146%	107.9	55.6	-51.5%
031	12	12	7.3	21.2	+290%	98.0	81.3	-17.0%
032	19	12	34.5	54.5	+157%	94.4	71.8	-23.9%

nature portfolio

Corresponding author(s): Olga Flamini and Christopher Janson

Last updated by author(s): Jul 18, 2025

Reporting Summary

Nature Portfolio wishes to improve the reproducibility of the work that we publish. This form provides structure for consistency and transparency in reporting. For further information on Nature Portfolio policies, see our Editorial Policies and the Editorial Policy Checklist.

Statistics

For all statistical analyses, confirm that the following items are present in the figure legend, table legend, main text, or Methods section.

n/a	Confirmed
☐	☒ The exact sample size (*n*) for each experimental group/condition, given as a discrete number and unit of measurement
☐	☒ A statement on whether measurements were taken from distinct samples or whether the same sample was measured repeatedly
☐	☒ The statistical test(s) used AND whether they are one- or two-sided *Only common tests should be described solely by name; describe more complex techniques in the Methods section.*
☐	☒ A description of all covariates tested
☐	☒ A description of any assumptions or corrections, such as tests of normality and adjustment for multiple comparisons
☐	☒ A full description of the statistical parameters including central tendency (e.g. means) or other basic estimates (e.g. regression coefficient) AND variation (e.g. standard deviation) or associated estimates of uncertainty (e.g. confidence intervals)
☐	☒ For null hypothesis testing, the test statistic (e.g. *F*, *t*, *r*) with confidence intervals, effect sizes, degrees of freedom and *P* value noted *Give P values as exact values whenever suitable.*
☒	☐ For Bayesian analysis, information on the choice of priors and Markov chain Monte Carlo settings
☒	☐ For hierarchical and complex designs, identification of the appropriate level for tests and full reporting of outcomes
☒	☐ Estimates of effect sizes (e.g. Cohen's *d*, Pearson's *r*), indicating how they were calculated

Our web collection on statistics for biologists contains articles on many of the points above.

Software and code

Policy information about availability of computer code

Data collection	No code used
Data analysis	Statistical Analysis System (SAS) Version 9.4 or higher and R Version 4.1.1 or higher were used to generate all statistical outputs.

For manuscripts utilizing custom algorithms or software that are central to the research but not yet described in published literature, software must be made available to editors and reviewers. We strongly encourage code deposition in a community repository (e.g. GitHub). See the Nature Portfolio guidelines for submitting code & software for further information.

Data

Policy information about availability of data

All manuscripts must include a data availability statement. This statement should provide the following information, where applicable:

- Accession codes, unique identifiers, or web links for publicly available datasets
- A description of any restrictions on data availability
- For clinical datasets or third party data, please ensure that the statement adheres to our policy

At the outset of the trial, we omitted a data sharing provision from the consent documents signed by participants. As a result, in accordance with our Ethics Committee policies, we are not authorized to release the raw data to the public. Furthermore, the study is still in progress. De-identified patient characteristics, safety, and preliminary efficacy data from raw datasets generated in this study are included in the paper. Requests for more information about the raw data are

subject to a confidentiality agreement with Myrtelle and must comply with applicable legal and regulatory requirements. Qualified researchers may request access to the trial information by contacting oflamini@myrtellegtx.com. The requests will be addressed within 120days, and data transfer agreement may be required.

Research involving human participants, their data, or biological material

Policy information about studies with human participants or human data. See also policy information about sex, gender (identity/presentation), and sexual orientation and race, ethnicity and racism.

Reporting on sex and gender	No effort was make to collect gender identity information from the children in the study. Their sex is reported.
Reporting on race, ethnicity, or other socially relevant groupings	All subjects were White. This is reported in the manuscript. No analyses based on race were performed. Country of origin is reported, but no analyses were done based on country of origin.
Population characteristics	ASPA genotype and diagnosis with typical Canavan Disease
Recruitment	Subjects were recruited online with non-profit partners and through clinicaltrials.gov. Therefore there is a potential bias towards including patients whose parent are computer literate and have access to the internet.
Ethics oversight	The protocol was approved by the Dayton Children's Hospital IRB

Note that full information on the approval of the study protocol must also be provided in the manuscript.

Field-specific reporting

Please select the one below that is the best fit for your research. If you are not sure, read the appropriate sections before making your selection.

☒ Life sciences ☐ Behavioural & social sciences ☐ Ecological, evolutionary & environmental sciences

For a reference copy of the document with all sections, see nature.com/documents/nr-reporting-summary-flat.pdf

Life sciences study design

All studies must disclose on these points even when the disclosure is negative.

Sample size	The study was powered for safety and efficacy on the basis of previous clinical data with brain NAA concentrations as the primary variable of interest. Using 0.5 as the standard deviation of differences in a two-tailed, 5% paired t-test, a sample size of 15 gave power exceeding 99% for differences in NAA concentrations of 2 to 3 mM, which we believe represents a clinically significant change. Although our power analysis suggested that a smaller sample size was sufficient, we anticipated multiple comparisons and the possibility of subject attrition, and planned to enroll and treat 24 subjects, with the possibility of dose escalation.
Data exclusions	Data were missing where one subjects guardians refused permission for one procedure. This is an interim analysis. Data after the cut off date were not included in the manuscript. We expect to include them in a later publication.
Replication	The procedure was performed on multiple subjects. Subjects of various ages were and will be enrolled to assess generalizability of the findings.
Randomization	This is an open-label trial. No randomization was done.
Blinding	This is an open-label trial. No blinding was done.

Reporting for specific materials, systems and methods

We require information from authors about some types of materials, experimental systems and methods used in many studies. Here, indicate whether each material, system or method listed is relevant to your study. If you are not sure if a list item applies to your research, read the appropriate section before selecting a response.

Materials & experimental systems

n/a	Involved in the study
☒	☐ Antibodies
☒	☐ Eukaryotic cell lines
☒	☐ Palaeontology and archaeology
☒	☐ Animals and other organisms
☐	☒ Clinical data
☒	☐ Dual use research of concern
☒	☐ Plants

Methods

n/a	Involved in the study
☒	☐ ChIP-seq
☒	☐ Flow cytometry
☐	☒ MRI-based neuroimaging

Clinical data

Policy information about clinical studies

All manuscripts should comply with the ICMJE guidelines for publication of clinical research and a completed CONSORT checklist must be included with all submissions.

Clinical trial registration	NCT04833907
Study protocol	Protocol was submitted with originally submitted paper.
Data collection	The study is ongoing. To ensure consistency of procedures and dose administration, the study was conducted at a single site, Dayton Children's Hospital in Dayton, Ohio, USA
Outcomes	The primary objective of the study was to assess the safety and tolerability of ICV dosing of MYR-101 in children with typical CD. This was done by collection of adverse events as well as collection of routine labs

Plants

Seed stocks	N/A
Novel plant genotypes	N/A
Authentication	N/A

Magnetic resonance imaging

Experimental design

Design type	Imaging was done using synthetic MRI (SyMRI) and quantitative MRI
Design specifications	Synthetic MRI (SyMRI, Linköping, Sweden) was used to assess quantitative changes in myelin volume, white matter volume, grey matter volume, intracranial volume, intraparenchymal volume, and brain parenchymal fraction over time with respect to administration of MYR-101. A radiographical suite of tools within SyMRI was used to measure these features as previously described. Standard T1- and T2-weighted MRI sequences, diffusion-weighted imaging, and gradient recalled echo were derived from SyMRI data and used for safety outcomes (i.e., absence of post-operative hemorrhage or other complications). Pre-operative MRI was additionally used for Stealth neuro-navigation. The quantitative MRI sequence used is a time efficient Multi-Dynamic Multi-Echo (MDME) sequence. In summary, the sequence uses a saturation-recovery sequence applied with two echo times and four averages. For each average, the slice acquisition order is changed, which results in four different inversion times. Both the phase and magnitude data are saved, and the data are used to fit the curves for the longitudinal (R1) and transversal (R2) relaxation rates and to obtain the proton density (PD) with background phase correction and a spin system simulation to compensate for the slice selective radio-frequency pulse profile effects. Postprocessing done using SyMRI produces quantitative R1, R2, and PD maps with correction for field inhomogeneities and partial volume effects (6). The SyMRI myelin quantification in turn is based on the R1, R2, and PD maps, where each voxel is modeled into four compartments (7), namely the myelin, cellular, free water, and excess parenchymal water partial volumes. This is accomplished through a voxel-wise least-squares fit that models the relaxation behavior of the dominant slow-decay component of R1 and R2 while accounting for the amplitude of the PD signal. The myelin partial volume has very fast relaxation rates and is not directly measurable but is instead estimated through its magnetization exchange and effect on the observable proton pool.

Behavioral performance measures	Subjects did not perform any tasks during imaging. Imaging was used to measure concentrations of NAA, myelin, white matter, and grey matter

Acquisition

Imaging type(s)	Standard MRI (structural), synthetic MRI
Field strength	3.0T
Sequence & imaging parameters	Conventional MRI uses standard pulse sequences (T1 and T2 weighted, FLAIR, GRE, DWI/ADC). SyMRI uses MDME sequence.Slice thickness 4 and 5 mm
Area of acquisition	Whole brain scan

Diffusion MRI ☐ Used ☒ Not used

Preprocessing

Preprocessing software	n/a (not functional MRI)
Normalization	SyMRI uses proprietary normalization techniques
Normalization template	n/a
Noise and artifact removal	na/
Volume censoring	n/a

Statistical modeling & inference

Model type and settings	n/a
Effect(s) tested	n/a

Specify type of analysis: ☐ Whole brain ☐ ROI-based ☐ Both

Statistic type for inference (See Eklund et al. 2016)	voxel-wise
Correction	n/a

Models & analysis

n/a	Involved in the study
☒	☐ Functional and/or effective connectivity
☒	☐ Graph analysis
☒	☐ Multivariate modeling or predictive analysis